

## Direct, Non-Destructive Imaging of Magnetization in a Spin-1 Bose Gas

J. M. Higbie, L. E. Sadler, S. Inouye, A. P. Chikkatur, S. R. Leslie,  
K. L. Moore, V. Savalli, and D. M. Stamper-Kurn  
Department of Physics, University of California, Berkeley CA 94720  
(Dated: March 23, 2004)

Polarization-dependent phase-contrast imaging is used to spatially resolve the magnetization of an optically trapped ultracold gas. This probe is applied to Larmor precession of degenerate and nondegenerate spin-1  $^{87}\text{Rb}$  gases. Transverse magnetization of the Bose-Einstein condensate persists for the condensate lifetime, with a spatial response to magnetic field inhomogeneities consistent with a mean-field model of interactions. Rotational symmetry implies that the Larmor frequency of a spinor condensate be density-independent, and thus suitable for precise magnetometry with high spatial resolution. In comparison, the magnetization of the noncondensed gas decoheres rapidly.

PACS numbers: 03.75.Gg, 05.30.Jp, 52.38.Bv

Quantum fluids with a spin degree of freedom have been of longstanding interest, stimulated both by the complex phenomenology of superfluid  $^3\text{He}$  [1] and by p-wave superconductivity [2]. Measurements of magnetization and magnetic resonance have been crucial to revealing the internal structure of these systems, inviting the application of such techniques to related fluids. Advances in ultracold atomic physics have now led to the creation of novel multi-component quantum fluids including pseudospin- $\frac{1}{2}$  Bose-Einstein condensates (BECs) [3] and spin-1 and -2 condensates of Na [4, 5] and  $^{87}\text{Rb}$  [6, 7, 8].

The internal state of a multi-component system is characterized by the populations in each of the components and the coherences among them. However, in all previous studies of the spin-1 or spin-2 spinor condensates, while the populations in each magnetic sublevel were measured, no information was obtained regarding the coherence between overlapping populations [4, 6, 7, 8, 9, 10]. Moreover, although spatial patterns of longitudinal magnetization have been reconstructed from images of freely expanding spinor gases, the expansion process severely limits the resolution obtainable [9, 11, 12].

In this work, we exploit atomic birefringence to image the magnetization of an ultracold spin-1 Bose gas non-destructively with high spatial resolution. By varying the orientation of an applied magnetic field with respect to our imaging axis, we measure either longitudinal magnetization, which derives from the static populations in each of the magnetic sublevels, or transverse magnetization, which derives from time-varying  $m = 1$  coherences. This probe is used to observe Larmor precession in both degenerate and non-degenerate spinor Bose gases. In particular, optical characterization of Larmor precession in a BEC provides a novel probe of the relative phases between condensates in different internal states with excellent temporal and spatial resolution (see Refs. [13] for other recent measurements of condensate phase).

This work is related to experiments by the JILA group in which either continuous [14] or pulsed [12] microwave fields were used to analyze a two-component (pseudospin- $\frac{1}{2}$ )  $^{87}\text{Rb}$  gas. However, unlike this pseudospin system, the

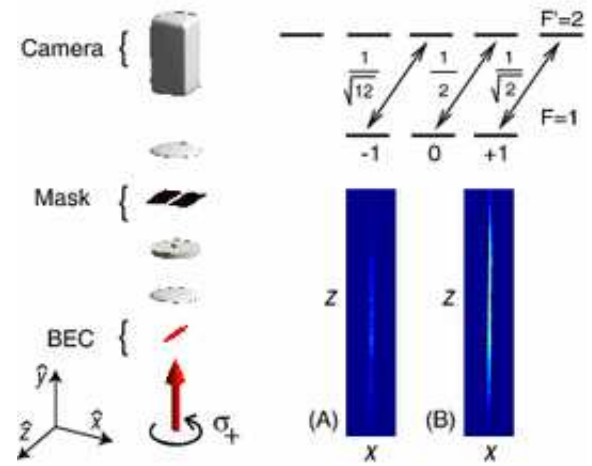


FIG. 1: Imaging system for direct detection of atomic magnetization. Left: Circularly polarized probe light illuminates the trapped gas. A first lens and phase dot form a primary phase-contrast image which is selectively masked and then reimaged by a second lens onto the camera as one of 40 frames which form a single composite image. Top right: Clebsch-Gordan coefficients for the imaging transition. Bottom right: Sample images of a BEC (a) with the atomic spin along  $\hat{y}$  and (b) with the spin along  $+\hat{y}$ , demonstrating the magnetization sensitivity of our technique. Higher-resolution version of figure at <http://physics.berkeley.edu/research/ultracold>

spin-1 spinor gas has more spin degrees of freedom and hence a richer state space, the spin orientation is connected directly with actual magnetization, and its internal degree of freedom possesses vector symmetry, implying the rotation invariance of its interactions. This rotational invariance manifests itself in our work in the gapless nature of "magnon" excitations, and in the density independence of the Larmor precession frequency.

Our probe relies on the phase-contrast technique which permits multiple-shot in-situ imaging of optically thick samples [15]. One can thus directly observe the dynamics of a single gaseous sample, rather than reconstructing them from experiments on many different samples.

The phase-contrast in aging signal strength for polarized probe light depends on both the density and the internal state of the atoms being imaged. In the case of imaging an  $F = 1$  gas of  $^{87}\text{Rb}$  with  $\sigma$  circularly polarized light near the  $F = 1 \rightarrow F = 2$  D1 transition, the phase-contrast signal is  $\frac{1}{4}n \left( \frac{2}{3} + \frac{5}{6}hF_y i + \frac{1}{6}hF_y^2 i \right)$  assuming that the optical susceptibility of the dilute gas is small. Here  $n$  is the column number density,  $\sigma = 3 \times 10^{-16} \text{ m}^2$  the resonant cross section,  $\Delta$  the probe detuning in half linewidths, and  $F_y$  the projection of the dimensionless atomic spin on the probe axis. The phase-contrast signal is thus largely a local measure of one vector component of the magnetization, when the density is known [16].

We perform our experiments by collecting  $5 \times 10^9$   $^{87}\text{Rb}$  Zeeman-slowed atoms in a magneto-optical trap, loading the cloud into a Ioffe-Pritchard magnetic trap and evaporatively cooling it to  $2 \text{ K}$ , before transferring the atoms into a single-beam, linearly-polarized optical dipole trap (ODT). The ODT derives from a free-running 825 nm diode laser, whose fiber-coupled output is focused to diffraction-limited beam waists of  $(w_x; w_y) = (39; 13) \text{ }\mu\text{m}$  at the trap. For the condensate studies, the ODT power is then ramped down over 700 ms from 12 mW to a nominal value of 2.3 mW, corresponding to trap frequencies  $(\omega_x; \omega_y; \omega_z) = 2\pi (150; 400; 4) \text{ s}^{-1}$  (axis orientations are indicated in Fig. 1). The resulting evaporation yields nearly pure condensates of  $4 \times 10^6$  atoms with a peak density of  $5 \times 10^{14} \text{ cm}^{-3}$ . For the studies of the thermal cloud, we hold the ODT power at 6.4 mW, yielding a gas of  $6 \times 10^6$  atoms at a temperature of  $1.1 \text{ K}$ , and a trap with frequencies  $(\omega_x; \omega_y; \omega_z) = 2\pi (250; 670; 7) \text{ s}^{-1}$ .

The atomic sample is phase-contrast imaged in two stages of magnification (6 and 2 sequentially) onto a CCD camera. A physical mask blocks illumination of all but a narrow slit-shaped region of the CCD chip. Taking advantage of a rapid frame-shifting mode of our camera, we record 40 consecutive images, each 25 pixels wide, at a rate of 20 kHz before uploading the images. We use probe light detuned 212 MHz below the  $F = 1 \rightarrow F = 2$  D1 transition ( $\lambda = 795 \text{ nm}$ ). Probe pulses are 5 s long with an average intensity of  $300 \text{ W cm}^{-2}$  [17].

We induce Larmor precession in our atomic sample starting with a spin-polarized gas in the  $F = 1; m_F = 1$  state and a bias field of 54 mG along the  $z$  direction [18]. A resonant RF pulse tips the spin vector by an angle  $\theta = 2$ . As the tipped spin precesses about the bias field, the phase contrast image intensities oscillate (Fig. 2a). We extract the peak signal from each of the 40 phase-contrast images by first binning in the  $z$  direction over a small region (27  $\mu\text{m}$  for the BEC and 108  $\mu\text{m}$  for the thermal cloud) at the center of the cloud, and then fitting to a sinc function in the radial ( $x$ ) direction to account for aberrations arising from imaging objects near the 6  $\mu\text{m}$  imaging resolution limit. The temporal oscillation in the peak height of our phase contrast images is clearly visible (Fig. 2b), and is present only after

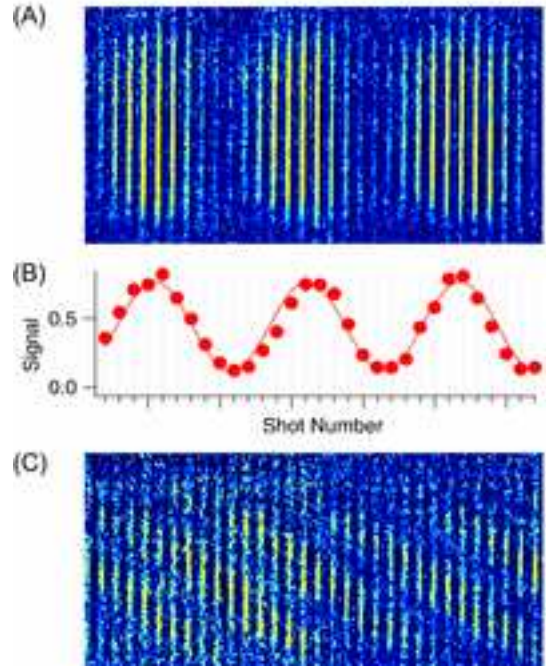


FIG. 2: Direct imaging of Larmor precession of a spinor BEC through magnetization-sensitive phase-contrast imaging. Shown are 31 consecutive images each with  $325 \times 18 \text{ }\mu\text{m}$  field of view. (a) Larmor precession is observed as a periodic modulation in the intensities of repeated images of a single condensate. (b) The peak signal strength oscillates at a rate which results from aliased sampling of a precisely measured  $38.097(15) \text{ kHz}$  Larmor precession at a sampling rate of  $20 \text{ kHz}$ . (c) In the presence of an  $8 \text{ mG/cm}$  axial gradient, images indicate "winding" of the transverse magnetization along the condensate. Images begin (a) 24.5 ms or (c) 14.5 ms after the tipping RF pulse. In (a), the field gradient is cancelled to less than  $0.2 \text{ mG/cm}$ . Higher-resolution version of figure at <http://physics.berkeley.edu/research/ultracold>

the RF pulse is applied. The transverse magnetization signals can be compared to those from the static longitudinal polarization of spin-polarized samples in the  $F = 1; m_F = 1$  states held in a magnetic field pointing along the imaging axis (Fig. 1). This comparison confirms that the Larmor-precessing samples are maximally polarized. We note that the ratio of 4.2 observed between the signals from spin-up and spin-down atoms is less than the theoretical value of 6, perhaps because of imperfect probe polarization.

The Larmor frequency of  $38 \text{ kHz}$  is chosen in order to maintain accurate control of the field direction and avoid unwanted spin flips due to low-frequency field noise in our laboratory. Since twice the  $20 \text{ kHz}$  frame rate of our images is within  $2 \text{ kHz}$  of the Larmor frequency, we observe an aliased low-frequency oscillation at the difference frequency. Combined with the less precise, but absolute, determination of the RF pulse resonance frequency, the Larmor precession signal measures in a single shot the instantaneous magnetic field to a fraction of a milligauss.

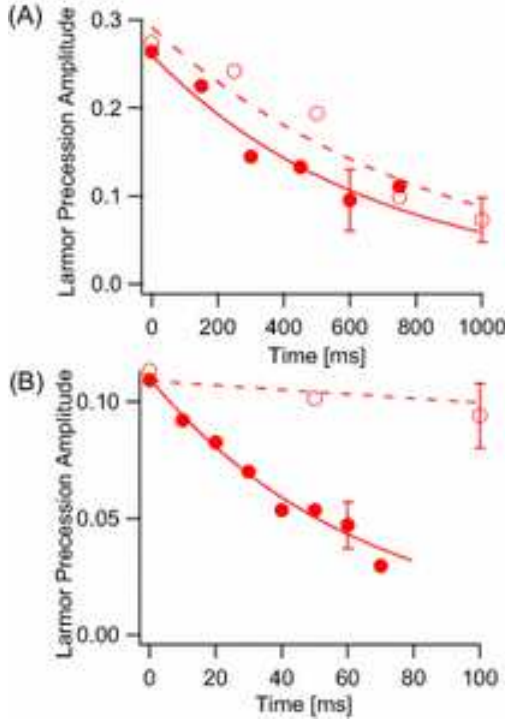


FIG. 3: Decay of the Larmor precession amplitude for (a) a BEC and (b) a thermal cloud. Data from the "tip and hold" (filled circles) or "hold and tip" (open circles) methods are compared (see text). The 1/e decay time of Larmor precession in a BEC was  $670 \pm 120$  ms, close to that of the "hold and tip" signal ( $830 \pm 120$  ms), indicating no decoherence source other than number loss. The  $65 \pm 10$  ms decay time of Larmor precession in a thermal cloud was an order of magnitude shorter than that of the "hold and tip" signal ( $1100 \pm 500$  ms).

The amplitude of the Larmor precession signal gives a quantitative measure of the coherence among Zeeman sublevels. Atomic gases with long-lived and well-characterized coherences have important scientific and technological applications. The lifetime of magnetic-field-insensitive hyperfine coherences in ultracold atoms has been studied [11, 19, 20], with coherence times up to 2 s reported. To measure the lifetime of Zeeman coherences in an ultracold Bose gas, we tip the atomic spin using an RF pulse, as before, and then wait a variable time before measuring the amplitude of the Larmor precession signal (the "tip and hold" method). To isolate effects that specifically diminish transverse magnetization from atom-number loss or other systematic effects, we alternatively reverse the order of the delay and the RF pulse ("hold and tip").

Results of such a measurement are shown in Fig. 3 [21]. The lifetime of transverse magnetization in a spinor BEC, taken as the 1/e time of an exponential fit to the precession amplitude vs. time, was  $670 \pm 120$  ms, compared to the measured  $830 \pm 120$  ms condensate lifetime (determined from the "hold and tip" method) in the optical trap. In other words, no significant decoherence occurs

other than that attributable to overall number loss, consistent with 3-body decay [22]. We note that on other repetitions of the experiment (data presented in Fig. 4), decoherence was observed on a timescale of about 400 ms, somewhat shorter than the condensate lifetime. We cannot presently account for this variation.

As the condensate is held for long times after the magnetization is tipped into the transverse plane, the Larmor precession signal begins to display a position-dependent phase shift (observed as high as 25 radians) along the condensate axis, attributable to magnetic field inhomogeneity (Fig. 2c). For example, a gradient of the field magnitude along the long axis of the condensate leads to a "corkscrew" transverse magnetization, which winds up over time (similar observations were made of pseudospin- $\frac{1}{2}$  spinor condensates [14]). Qualitatively, the condensed gas behaves as if its constituent atoms were frozen in place, precessing at a frequency given by the local value of the inhomogeneous magnetic field.

The response of the condensate magnetization to magnetic field inhomogeneities can be described by the separate motion of each of the three magnetic components present in a transversely polarized cloud. A magnetic field gradient imposes, over short times, a  $e^{im\phi}$  relative phase (or in parts a  $m \sim q$  relative momentum) on the three components, labelled by the magnetic quantum number  $m$ . This defines a "corkscrew" magnetization with pitch  $2\pi/q$ . At longer times, the inhomogeneous trapping potential and condensate density begin to influence the motion of the separate components, and hence the magnetization orientation. For example, in a harmonically confined non-interacting spinor BEC, one would expect the following evolution in successive quarter cycles of harmonic motion: magnetization winding up, unwinding, winding up in the opposite sense, and unwinding again. However, we observe no such dynamics, finding the phase of Larmor precession at different portions of the condensate to advance linearly with time through the 250 ms axial oscillation period. This behavior, at least for the case of slight inhomogeneities, can be explained by noting that slight rotations of the magnetization orientation are associated with magnons possessing a gapless and free-particle-like spectrum above the chemical potential, which is constant across the condensate [23]. Thus, for an interacting spinor condensate, the combined effect of the inhomogeneous condensate mean-field energy and the trap potential is to cause magnons, and hence small-scale magnetization rotations, to advance as if no external potential were present. We expect this argument to apply similarly to larger variations of the magnetization orientation, in accordance with our observations.

In contrast, transverse magnetization in a non-degenerate spinor gas decays much faster than that in a BEC (Fig. 3). Moreover, the Zeeman decoherence rate in a thermal gas depends strongly on the applied magnetic field gradient (Fig. 4), while the (local) Zeeman coherence in a BEC is unaffected by similar inhomogeneities.



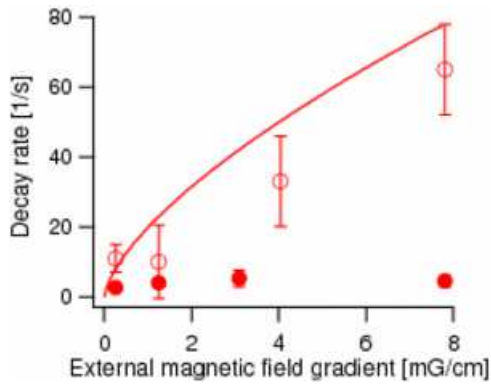


FIG. 4: Dependence of Larmor precession decay rate on applied gradient. Decay rates for the condensate are represented by filled circles and for the thermal cloud by open circles. The solid curve is a theoretical prediction for the thermal cloud precession decay rate, as discussed in the text.

For Fig. 4 we calibrated the axial field gradient by fitting for the phase of the Larmor precession at different axial positions in a condensate. We can use this information to cancel the axial gradient at the center of the trap to better than  $0.2 \text{ mG/cm}$ , at which stage higher-order inhomogeneities, most notably a field curvature of about  $20 \text{ mG/cm}^2$ , dominate. More generally, this method may allow for precise magnetometry with high spatial resolution ( $\sim 10 \text{ nm}$ ).

The decay rates of transverse magnetization in a thermal cloud may be estimated simply as  $\tau_{LP}^{-1} = (\frac{1}{2} v_{th}^2 n_c)^{1/3}$ , where  $\tau_{LP}$  is the time for an atom to diffuse [24] into a field large enough to dephase its spin by  $\pi$  relative to a stationary spin,  $v_{th}$  is the mean thermal velocity,  $n$  the number density,  $\sigma_c$  the collisional cross-section, and  $2\pi \hbar \vec{\mu}_B$  the magnetic gradient. This simple result is shown in Fig. 4 to agree fairly well with measurement. We note that this simple picture neglects spin waves, which were observed in pseudospin- $\frac{1}{2}$  gases [11, 12, 25] and which should exist (in modified form) in

spin-1 Bose gases as well.

The demonstrated ability to image directly the magnetization of a spinor Bose gas and the observation of long-lived Zeeman coherences point to a number of future investigations. Given the quadratic dependence of the dominant 3-body loss rate on condensate density, much longer Zeeman coherence times may be attained in lower-density spinor BECs. Furthermore, one expects the Larmor precession frequency of a spinor BEC to be density independent at low magnetic fields. This result stems from the vectorial symmetry of the atomic spin, which requires the zero-field interatomic interactions to be rotationally invariant [23]. Consequently, spinor BECs constitute an attractive system for precise magnetometry. Moreover, such magnetometry may be regarded as a form of condensate-based interferometry, and as such invites similar questions regarding the stability of the condensate phase, e.g. due to interactions [26] or reduced dimensionality [27]. The fact that imaging the transverse magnetization of a spin-1 gas resolves spatially-varying phase relations among three condensed components opens new experimental opportunities.

Our imaging method also promises to illuminate the mostly unexplored properties of spinor condensates. For example, spin-1 condensates of  $^{87}\text{Rb}$  are predicted to be ferromagnetic [23, 28]. While measurements of populations of the magnetic sublevels are consistent with this prediction [6, 7], no information on coherences, and thus no conclusive evidence of ferromagnetism, has been obtained. We are presently attempting to detect the spontaneous Larmor precession of a  $^{87}\text{Rb}$  condensate as it relaxes to a ferromagnetic ground state. These experiments will be described elsewhere.

We thank F. Lienhart, M. Pasienski, E. Crump and the UCB Physics Machine and Electronics Shops for assistance, and W. Ketterle and D. Budker for helpful comments. This work was supported by the NSF, the Hellman Faculty Fund, and the Alfred P. Sloan and the David and Lucile Packard Foundations. KLM acknowledges support from the NSF and SRL from the NSERC.

[1] D. Vollhardt and P. Wölfle, *The Superfluid Phases of Helium 3* (Taylor and Francis, New York, 1990).  
[2] A. P. M. Ackenize and Y. M. Aeno, *Rev. Mod. Phys.* **75**, 657 (2003).  
[3] D. S. Hall et al., *Phys. Rev. Lett.* **81**, 1543 (1998).  
[4] J. Stenger et al., *Nature* **396**, 345 (1998).  
[5] A. G. Orlov et al., *Phys. Rev. Lett.* **90**, 090401 (2003).  
[6] H. Schmalthann et al., *Phys. Rev. Lett.* **92**, 040402 (2004).  
[7] M.-S. Chang et al., *Phys. Rev. Lett.* **92**, 140403 (2004).  
[8] T. Kuwamoto et al., *Phys. Rev. A* **69**, 063604 (2004).  
[9] H.-J. Miesner et al., *Phys. Rev. Lett.* **82**, 2228 (1999).  
[10] D. M. Stamper-Kurn et al., *Phys. Rev. Lett.* **83**, 661 (1999).

[11] H. J. Lewandowski et al., *Phys. Rev. Lett.* **88**, 070403 (2002).  
[12] J. M. McGuirk et al., *Phys. Rev. Lett.* **89**, 090402 (2002).  
[13] Y. J. Wang et al., preprint, *arXiv cond-mat/0407689*; M. H. Wheeler et al., *Phys. Rev. Lett.* **93**, 170402 (2004); M. Saba et al., preprint (2005).  
[14] M. R. Matthews et al., *Phys. Rev. Lett.* **83**, 3358 (1999).  
[15] For application to BECs see M. R. Andrews et al., *Phys. Rev. Lett.* **79**, 553 (1997).  
[16] I. Carusotto and E. J. Mueller, *J. Phys. B* **37**, S115 (2004).  
[17] Probe light at  $300 \text{ W/cm}^2$  in parts state-dependent AC Stark shifts equivalent to a  $0.6 \text{ mG}$  field along the probe direction. We observed no spin flips or number loss from

our sample from this pulsed field.

- [18] After nulling the magnetic field to  $< 5$  mG, we apply additional field either along or orthogonal to the imaging axis. Remaining field fluctuations cause shot-to-shot rms variations of 1.6 kHz in the Larmor precession frequency.
- [19] D. M. Harber et al., Phys. Rev. A 66, 053616 (2002).
- [20] N. Davidson et al., Phys. Rev. Lett. 74, 1311 (1995).
- [21] Here we fit the oscillation independently in each of three contiguous 27 m binning regions and then average the three amplitudes obtained.
- [22] E. A. Burt et al., Phys. Rev. Lett. 79, 337 (1997).
- [23] T.-L. Ho, Phys. Rev. Lett. 81, 742 (1998); T. Ohmachi and K. Machida, J. Phys. Soc. Jpn. 67, 1822 (1998).
- [24] Due to the large collision rate (200 Hz) compared with the axial oscillation frequency (7 Hz), thermal atoms move diffusively and slower than they would ballistically; also noted in Ref. [19].
- [25] N. P. Bigelow et al., Phys. Rev. Lett. 63, 1609 (1989).
- [26] M. Greiner et al., Nature 419, 51 (2002).
- [27] S. Dettmer et al., Phys. Rev. Lett. 87, 160406 (2001).
- [28] N. N. Klausen et al., Phys. Rev. A 64, 053602 (2001).